Electronic Supplementary Material (EIS) for

Atomically Precise Growth of Sodium Titanates as Anode Materials for High-Rate and Ultralong Cycle-Life Sodium-Ion Batteries

Jian Liu,[a,b] Mohammad N. Banis,[a] Biwei Xiao,[a] Qian Sun,[a] Andrew Lushington,[a] Ruying Li,[a] Jinghua Guo,[b] Tsun-Kong Sham,[c] and Xueliang Sun [a,]*

[a] Department of Mechanical and Materials Engineering, University of Western Ontario, London, Ontario N6A 5B9, Canada

[b] Advanced Light Source, Lawrence Berkeley National Laboratory, Berkeley, California 94720, United State

[c] Department of Chemistry, University of Western Ontario, London, Ontario N6A 5B7, Canada

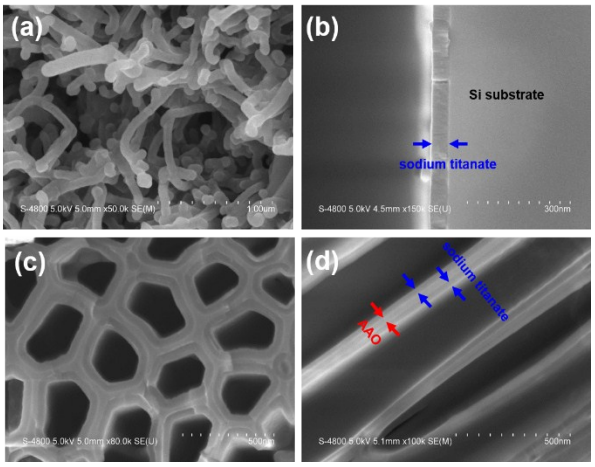

Fig. S1. Low-magnification SEM images of sodium titanate thin films deposited on (a) nitrogen-doped CNTs using 200 cycles, (b) Si (100) wafer using 400 cycles, and (c,d) AAO template using 200 cycles (top and cross-section views). The deposition was performed at 250 °C using ALD recipe of (NaO^tBu-H_2O) + (TTIP-H_2O).

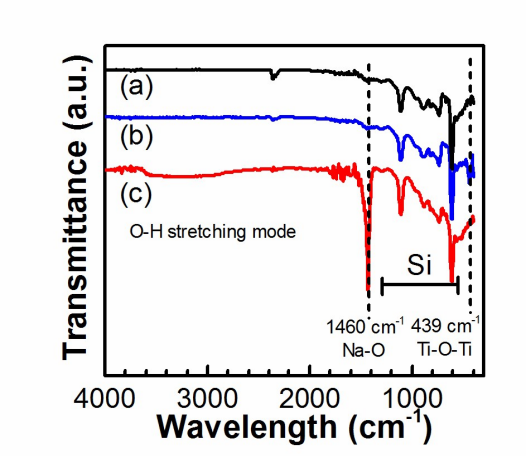

Fig. S2. FTIR spectra of (a) bare double-side polished Si wafer, (b) anatase TiO_2 deposited by ALD at 225 °C, and (c) sodium titanate deposited by ALD at 225 °C on double-side polished Si wafer. The sharp peak located at 1460 cm^{-1} in (c) is attributable to the formation of Na-O bonds in the sodium titanate films [1]. The peak centered at 439 cm^{-1} in (b) is ascribed to Ti-O-Ti bonds typically observed in anatase TiO_2 [2]. Disappearance of 439 cm^{-1} peak in (c) indicates the breaking of Ti-O-Ti bonds and formation of Na-O-Ti bonds in the sodium titanate films. Peaks from 605 cm^{-1} to 1105 cm^{-1} result from double-side polished Si wafer.

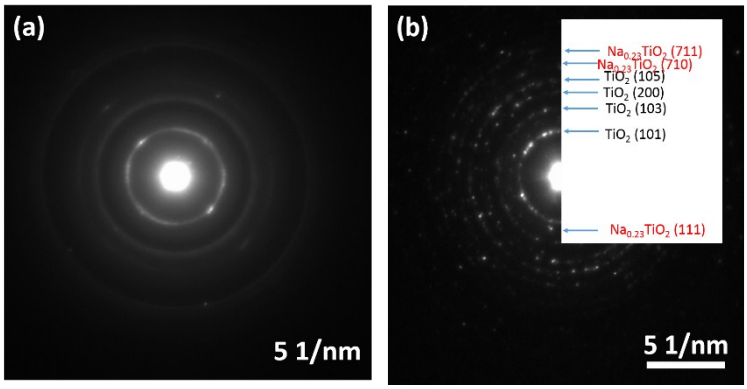

Fig. S3. Selected-area electron diffraction (SAED) patterns of (a) sodium titanates as-deposited on CNTs at 225 °C, and (b) sodium titanates/CNTs annealed at 500 °C in air.

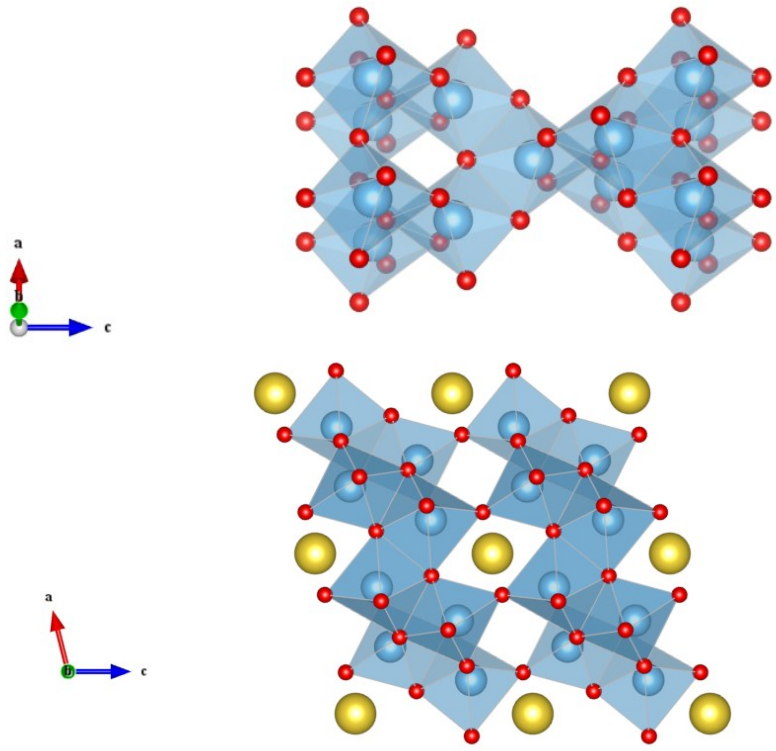

Fig. S4. Crystal structure of anatase TiO_2 (top) and $Na_{0.23}TiO_2$ (bottom) viewed along the *b*-axis. Red spheres represent oxygen, blue spheres represents titanium ions, yellow spheres represent sodium ions, and blue polyhedrons represent the Ti – O octrahedra.

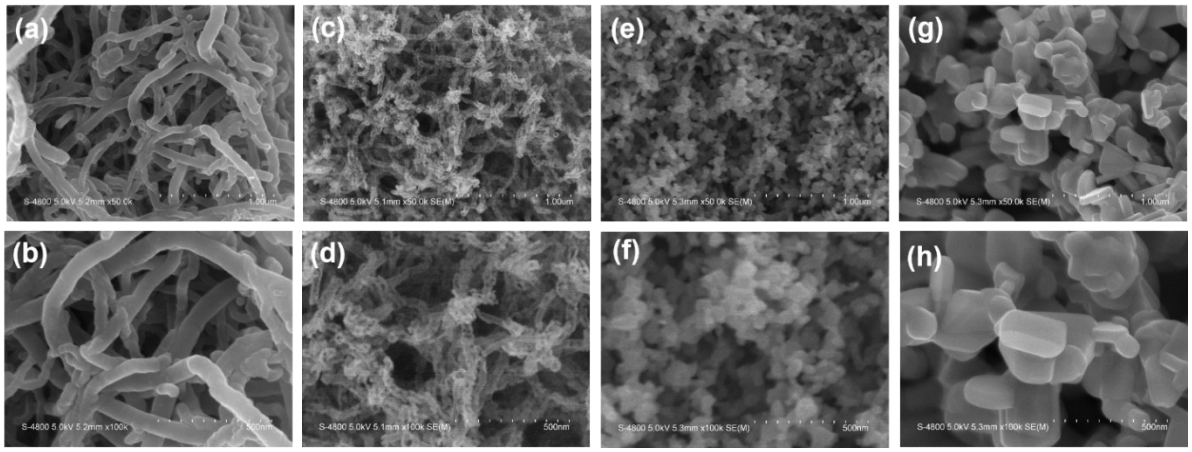

Fig. S5. SEM images of sodium titanates (a,b) as-deposited at 225 °C, after annealing in air at (c,d) 500 °C, (e,f) 700 °C, and (g,h) 900 °C, respectively.

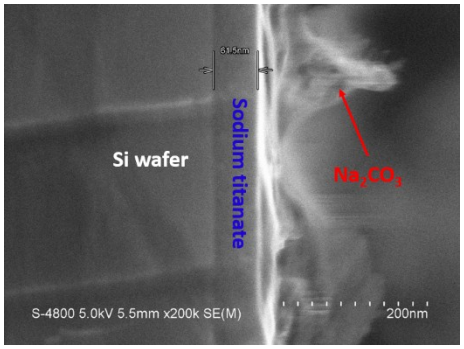

Fig. S6. Cross-section SEM image of sodium titanates deposited on Si wafer at 275 °C using 400 ALD cycles.

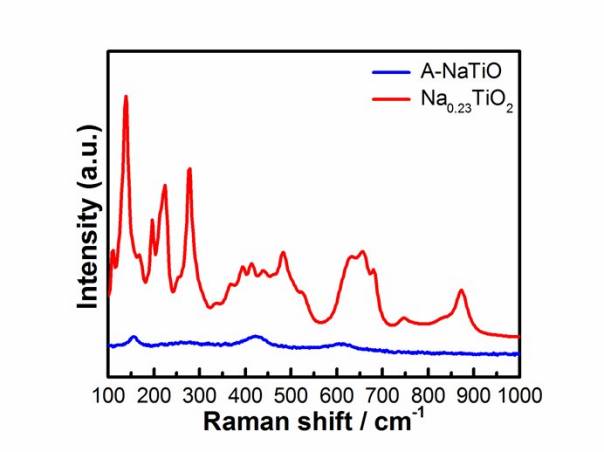

Fig. S7. Raman spectra of A-NaTiO and $Na_{0.23}TiO_2$. Raman bands below 278 cm^{-1} can be assigned to lattice modes and Na-O-Ti stretching vibration modes [3]; Raman bands between 370 and 484 cm^{-1} can be assigned to framework of Ti-O-Ti vibrations [4]; Raman bands between 632 and 683 cm^{-1} are due to the Ti-O-Ti stretch in edge-shared TiO_6 [1, 3-5]; Raman band at 873 cm^{-1} can be assigned to the symmetric stretch of short Ti-O bonds involving non-bridging oxygen atoms associated with sodium ions [1,4,5].

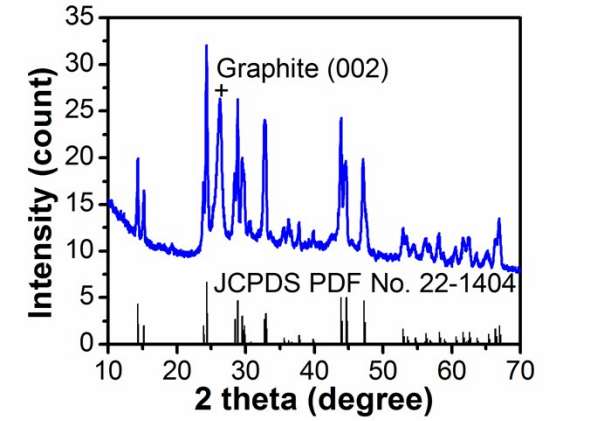

Fig. S8. XRD pattern of $Na_{0.23}TiO_2$/CNT composite prepared by annealing amorphous sodium titanates in argon gas for 10h.

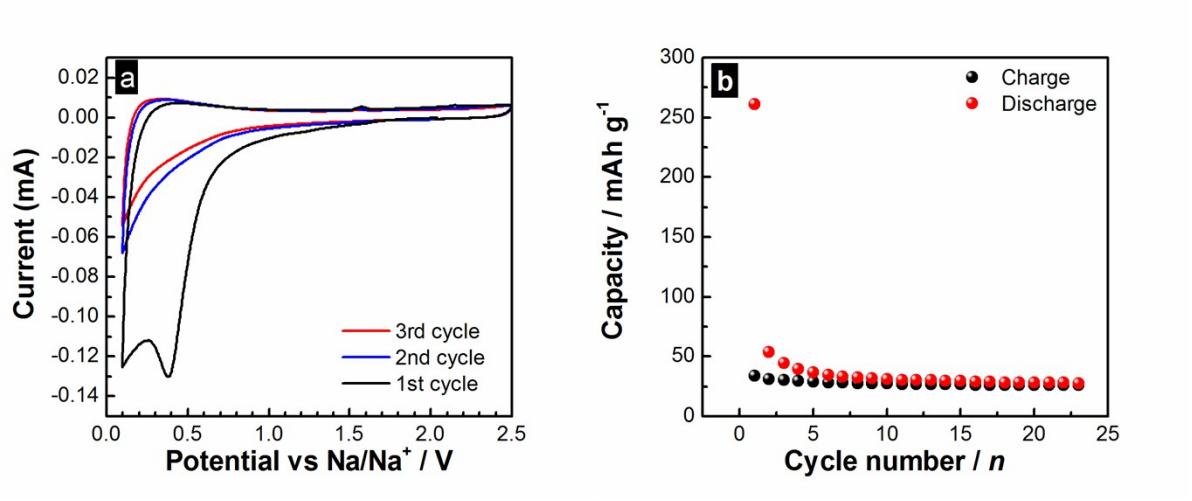

Fig. S9. (a) CV curve of pristine CNTs measured between 0.1 to 2.5V at a scanning rate of 0.1 mV s^{-1}; and (b) cycling performance of pristine CNTs at a current rate of 10 mA g^{-1}.

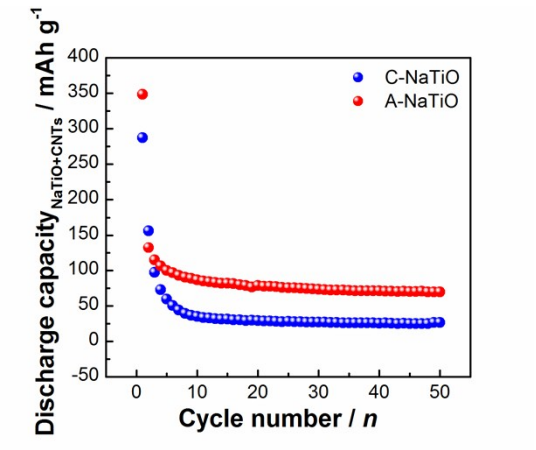

Fig. S10. Discharge capacity of A-NaTiO/CNT and C-NaTiO/CNT composites at a current rate of 10 mA g^{-1}.

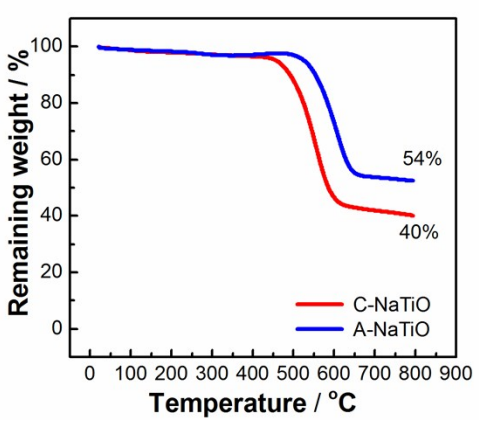

Fig. S11. TG results of A-NaTiO and C-NaTiO on CNTs as measured in air atmosphere at a heating rate of 30 ° min^{-1}.

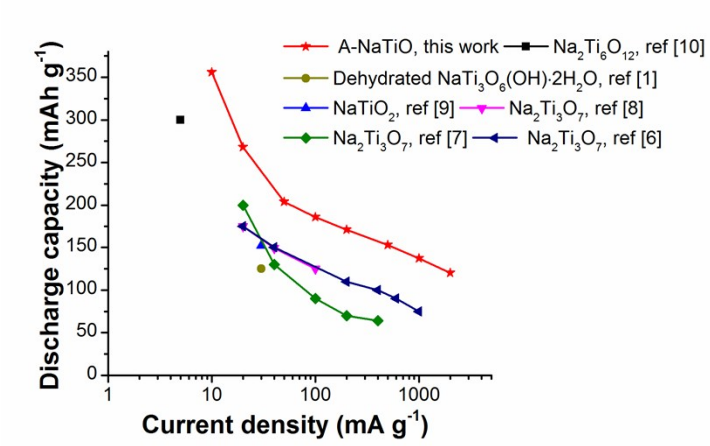

Fig. S12. Rate capability of A-NaTiO in this work in comparison with other types of sodium titanates reported in reference [1, 6-10]. At each current density, the discharge capacity of each sample was taken at the second cycle for comparison.

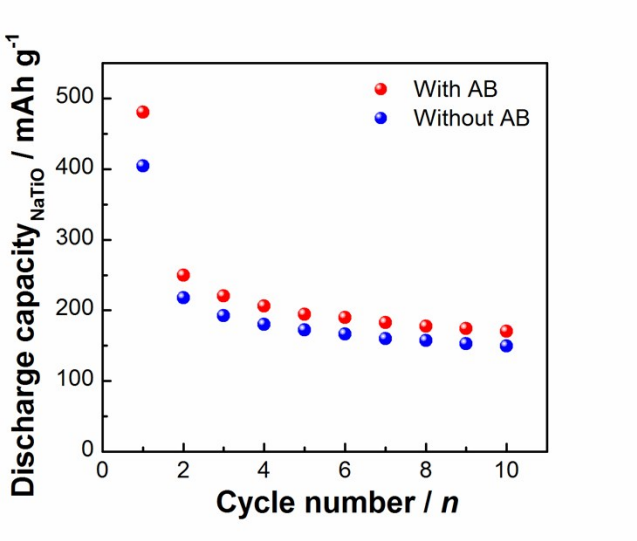

Fig. S13. Cycling stability of A-NaTiO/CNT electrodes prepared with acetylene black (AB) (A-NaTiO/CNTs:PVDF:AB = 8:1:1) and without AB (NaTiO/CNTs:PVDF = 9:1) at a current density of 10 mA g^{-1}.

References

1 M. Shirpour, J. Cabana and M. Doeff, *Energy Environ. Sci.* 2013, **6**, 2538-2547.

2 P. Vitanov, A, Harizanova and T. Ivanova, *J. Phys. Conf. Ser.* 2012, **356**, 012041.

3 B. C. Viana, O. P. Ferreira, A. G. Souza Filho, J. M. Filho and O. L. Alves, *J. Braz. Chem. Soc.* 2009, **20**, 167-175.

4 Z. Zhang, J. B. M. Goodall, S. Brown, L. Karlsson, R. J. H. Clark, J. L. Hutchison, I. U. Rehman and J. A. Darr, *Dalton Trans.* 2010, **39**, 711-714.

5 T. Gao, H. Fjellvåg and P. Norby, *Inorg. Chem.* 2009, **48**, 1423-1432.

6 A. Rudola, K. Saravanan, C. W. Mason and P. Balaya, *J. Mater. Chem. A* **2013**, *1*, 2653-2662.

7 H. Pan, X. Lu, X. Yu, Y.-S. Hu, H. Li, X.-Q. Yang and L. Chen, *Adv. Energy Mater.* **2013**, *3*, 1186-1194.

8 W. Wang, C. Yu, Y. Liu, J. Hou, H. Zhu and S. Jiao, *RSC Adv.* **2013**, *3*, 1041-1044.

9 S. Wu, X. Li, B. Xu, N. Twu, L. Liu, and G. Ceder, *Energy Environ. Sci.* **2015**, *8*, 195-202.

10 K. Shen and M. Wagemaker, *Inorg. Chem.* **2014**, *53*, 8250-8256.